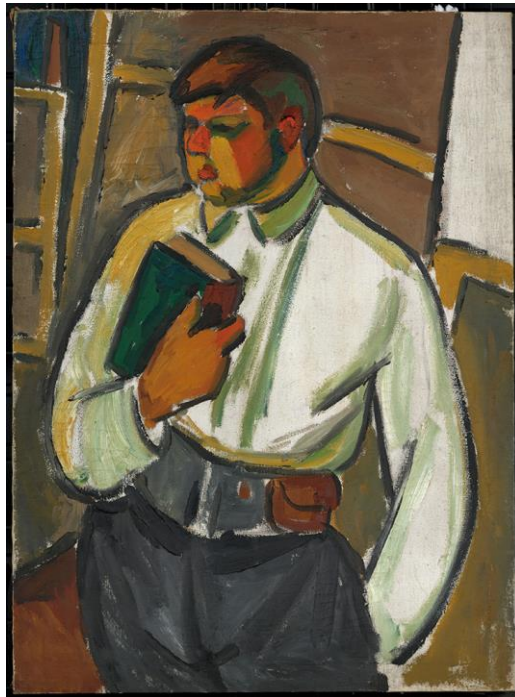


ANALYTICAL REPORT

[Ref.: AAR0955.J / 8 May 2018]



Portrait of a Man (Anton Beswal), 1910
Mikhail Larionov
Collection Museum Ludwig, Cologne, Inv. ML 1306

Art Analysis & Research Inc.
Ground Floor West, 162-164 Abbey Street, London SE1 2AN
T: +44 (0) 20 7064 1433
VAT Reg. No. 252 4541 22



Summary

A painting on canvas by Mikhail Larionov, *Portrait of a Man (Anton Beswal)*, belonging to the Museum Ludwig (reference: ML 1306), that has been dated to 1910 (it is unsigned and undated), was examined and analysed by Art Analysis & Research, Ltd. in cooperation with the Museum Ludwig, and funded through a grant from The Russian Avant Garde Research Project (RARP). This artwork formed a part of a group of fourteen well-provenanced paintings by the Russian artist couple Natalia Goncharova and Larionov, held in the collection of the Museum Ludwig that comprised the focus of this work. The goal set for this research was to investigate these paintings in order to characterise similarities and differences, with the objectives of 1) providing detailed studies of the specific paintings, 2) obtaining wider information on the artists' methods, 3) defining a blueprint for promising methodologies to develop further on other works by these artists and with an aim of applying such information in support a *catalogue raisonné*, and 4) creating the foundation for applying similar methodologies and techniques to other artists of the genre. To this end, each of the paintings are described in individual reports (as here) accompanied by a summary report under separate cover. The results of the program of examination, material analysis and technical imaging will be set out herein.



Contents

Summary	2
Tables, Figures and Plates.....	4
A. Introduction.....	6
B. Examination, imaging and analysis of the images	7
B.1 Methodology	7
B.2 General observations	7
B.3 Imaging.....	8
B.3.i Photography with ultraviolet illumination	8
B.3.ii Surface conformation	8
B.3.iii Short-wave infrared (SWIR).....	9
B.3.iv X-radiography and weave analysis	9
C. Sampling and analysis	10
C.1 Introduction	10
C.2 Support	11
C.3 Radiocarbon dating.....	11
C.4 Ground.....	12
C.5 Underdrawing.....	12
C.6 Paint layers: Pigments	12
C.7 Paint layers: Binding media	13
C.8 Stratigraphy	13
D. Discussion of the findings	14
D.1 Support, ground and preparatory work	14
D.1.i The support	14
D.1.ii Priming.....	15
D.1.iii Underdrawing	15
D.2 Paint, pigments and binding media	16
D.2.i General observations.....	16
D.2.ii Paint: pigment and binding medium	16
D.2.iv Materials analysis and implications for dating	17
E. Conclusions	18
F. Acknowledgements.....	19
G. Appendices	20

App.1 Sampling and sample preparation	20
App.1.i. Sampling	20
App.1.ii Cross-sectional analysis	21
App.2 Materials analysis summary results	21
App.2.i SEM-EDX, Raman microscopy and PLM analysis	22
App.2.ii Fourier Transform Infrared Spectroscopy-Attenuated Total Reflectance (FTIR-ATR)	23
App.2.iii Gas Chromatography-Mass Spectrometry (GCMS) Analysis	25
App.2.iv SYPRO® Ruby protein staining	25
App.2.v Canvas fibre identification	26
App.2.vi Radiocarbon measurement	26
App.3 Imaging methods	28
App.4 Plates	29
App.5 Cross-sections	45

Tables, Figures and Plates

Table App.1.i Samples taken for analysis	20
Table App.2.i Analytical results SEM-EDX, Raman Microscopy and PLM	22
Table App.2.ii Summary results from FTIR	23
Table App.2.iii Summary results from GCMS	25
Table App.2.iv SYPRO® Ruby stain results for sample [16].	25
Table App.2.v Canvas fibre identification	26
Table App.2.vi.i Radiocarbon measurement	27
Figure App.2.vi.ii Radiocarbon determination.	27
Plate 1. Mikhail Larionov, Portrait of a Man (Anton Beswal), c. 1910, collection Museum Ludwig: Inv. Nr. ML 1306. Recto, visible light.	29
Plate 2. Mikhail Larionov, Portrait of a Man (Anton Beswal), c. 1910, collection Museum Ludwig: Inv. Nr. ML 1306. Recto, UV light.	30
Plate 3. Mikhail Larionov, Portrait of a Man (Anton Beswal), c. 1910, collection Museum Ludwig: Inv. Nr. ML 1306. Recto, oblique illumination.	31
Plate 4. Mikhail Larionov, Portrait of a Man (Anton Beswal), c. 1910, collection Museum Ludwig: Inv. Nr. ML 1306. Recto, 3D laser scan.	32
Plate 5. Mikhail Larionov, Portrait of a Man (Anton Beswal), c. 1910, collection Museum Ludwig: Inv. Nr. ML 1306. Verso, visible light.	33
Plate 6. Mikhail Larionov, Portrait of a Man (Anton Beswal), c. 1910, collection Museum Ludwig: Inv. Nr. ML 1306. Verso, UV light.	34
Plate 7. Mikhail Larionov, Portrait of a Man (Anton Beswal), c. 1910, collection Museum Ludwig: Inv. Nr. ML 1306. Recto, SWIR image.	35
Plate 8. Detail of underdrawing, recto.	36

Plate 9. Recto, detail, drawing, upper proper left arm.....	37
Plate 10.a Mikhail Larionov, Portrait of a Man (Anton Beswal), c. 1910, collection Museum Ludwig: Inv. Nr. ML 1306. X-ray image	38
Plate 10.b The X-ray image before digital compensation for the stretcher bars.	39
Plate 11.a Maps showing variation in canvas thread angle.....	39
Plate 12.a Detail of canvas, verso.	41
Plate 12.b Detail of canvas, right tacking margin, showing selvedge, right, along top edge.	41
Plate 12.c Detail of canvas, right tacking margin, showing selvedge.	41
Plate 13.a Microscope detail of the lead white-based priming on the canvas, recto.....	42
Plate 13.b Detail of the black material that may form the laying in, or ‘underdrawing’.	42
Plate 13.c Detail of the cusping of the exposed, primed canvas along the tacking margins.....	42
Plate 14.a Macro detail of the brittle cracking and granular nature of some of the painting’s surface.	43
Plate 14.b Detail of protrusions from the underlying layer, projecting through the overlying brown.	43
Plate 14.c Macro detail of the brittle cracking of the paint film.	43
Plate 15. Image showing approximate location of samples taken for materials analysis.	44
Plate 16. Cross-section, Sample [15].....	45
Plate 17. Cross-section, Sample [15].....	45
Plate 18. Cross-section, Sample [16].....	46
Plate 19. Cross-section, Sample [16].....	46
Plate 20. Cross-section, Sample [16], stained with SYPRO [®] Ruby.	47

A. Introduction

The painting known as *Portrait of a Man (Anton Beswal)* (**Plate 1**) by the artist Mikhail Larionov (1881-1964), a work on canvas measuring 1095 mm high by 880 mm wide, is now part of the collection of the Museum Ludwig, Cologne (Inv. ML 1306). It is unsigned and undated; a date of 1910 has been proposed for its creation. It has been examined as part of a larger technical study of fourteen paintings by Natalia Goncharova and Larionov in the Museum Ludwig, as part of a project funded through a grant from the charity the Russian Avant Garde Research Project (RARP). The project goal has been to generate detailed technical profiles on authentic paintings by Goncharova and Larionov to expand the data available for art historical study and technical characterization of their work¹; consequently, fourteen well-provenanced paintings by the Russian artist couple held in the collection of the Museum Ludwig were thoroughly examined and analysed². The short-term goal of the project was to define a blueprint for promising routes of research to develop further on other works by these artists and with a long-term goal of contributing such information to support a technical *catalogue raisonné*; these recommendations are laid out in a summary report³.

The information in this report therefore provides a detailed technical and material account of the painting. In addition, this is considered in light of the conservation history and provenance information relating to the painting, held by the Museum Ludwig; the supplementary reports produced by Verena Franken in the course of her work on the RARP project summarises this material⁴. Some of the information concerning examination of the painting has been included here, as relevant, as are a representative selection of the extensive documentation photographs she made.

The structure of this report is as follows. First, the primary findings of the visual examination and technical imaging will be described in **Section B**.

Materials analysis on micro-samples taken for pigment and binding medium identification and cross-sections is described in **Section C**.

¹ There is limited specific information available. This includes: Rioux, J.-P.; Aitken, G.; Duval, A. 'Étude en laboratoire des peintures de Gontcharova et Larionov', pp. 220-223. In: *Nathalie Gontcharova, Michel Larionov* [exh. cat.], Éditions du Centre Pompidou : Paris (1995). Rioux, J.-P.; Aitken, G.; Duval, A. 'Matériaux et techniques des peintures de Nathalie S. Gontcharova et Michel F. Larionov du Musée national d'art moderne', *Techne* **8** (1998) 7-32. Gallone, A. 'Œuvres de Michel Larionov et Nathalie Gontcharova: Analyse de la Couleur', *Le dessin sous-jacent la technologie dans la peinture: Colloque XI 14-16 septembre 1995*, R. Van Schoute and H. Verougstraete (eds), Louvain-la-Neuve (1997) pp. 137-141, Pl. 74-76.

² These include: Natalia Goncharova: *Paysage de Tiraspol (Tiraspol Landscape)*, 1905, ML 01483; *Rusalka*, 1908, ML 1304; *Still Life with Tiger Skin*, 1908, ML 1305; *The Jewish Family*, 1912, ML 1369; *The Orange Seller*, 1916, ML 1484; *Portrait of Larionov*, 1913, ML 1319.

Mikhail Larionov, *Still Life with Coffee Pot*, c. 1906, ML 01486; *Still Life*, c. 1907/1912, ML 1487; *Still Life with a Crayfish (Nature morte à l'écrevisse)*, c. 1907, ML 1331; *Portrait of a Man*, c. 1910, ML 1306; *Rayonism, Red and Blue (Beach)*, 1911, ML 1333; *Saucisson et maquereau rayonnists (Rayonistic Sausage and Mackerel)*, 1912, ML 1307; *Venus*, 1912, ML 1332; *Rayonistic Composition*, inscribed 1916, ML/Z 211/134.

³ *Summary Report of the RARP Goncharova/Larionov Project, with the Museum Ludwig*, Art Analysis & Research Inc. (2017).

⁴ See reports: *AAR0955.J ML 1306 Conservation*, Franken, V. 'Report on the examination of the painting *Portrait of a Man* (1910) by Mikhail Larionov' (2017a) and *AAR0955.J ML 1306 Archives*, Franken, V. 'Report on the content of the Museum Ludwig archives, concerning the painting *Portrait of a Man* (1910) by Mikhail Larionov' (2017b).

Inferences drawn regarding the painting on the basis of these investigations will be discussed in **Section D**.

The methodologies and protocols used in each case may be found described in the general **Protocols** supplement, appended to this series of reports.

B. Examination, imaging and analysis of the images

B.1 Methodology

The painting was initially examined visually under normal lighting conditions and with ultraviolet light (UV), then with a stereo binocular microscope.

A range of technical imaging techniques were also employed (**Appendix 3**), generating a variety of images and imaging datasets⁵. These are presented as follows:

- High-resolution visible colour (**Plates 1, 5**);
- UV luminescence (**Plates 2, 6**);
- Oblique illumination (**Plate 3**);
- 3D laser surface scanning (**Plate 4**);
- Short-wave infrared (SWIR), 1600-2500nm (**Plates 7, 8**);
- X-radiography (**Plate 10**).

Additionally, weave analysis (including thread counting) was conducted on the basis of the X-radiograph (**Plates 11.a-d**). Some exemplar images recorded as part of the surface microscopy and macrophotography are also reproduced here (**Plates 12-14**).

The imaging revealed a range of aspects regarding the use of materials, structure and technique of production of the painting that are complementary to the visual observations made. Consequently, specific observation will be made to each in this section regarding the interpretation of these specific forms of analysis, while a summary overview in the context of the painting technique is presented in **Section D**, below.

B.2 General observations

The painting is executed on canvas, which has not been lined, so that both the recto and the verso of the artwork could be studied. It is not, however, on its original stretcher, having been restretched onto a newer, secondary support. The painting is in good condition, with minor, localised retouching where there have been small losses of paint, particularly along the upper edge. The paint and ground are somewhat matt, suggesting a low concentration of binding medium, and are

⁵ Additionally, a visible-NIR multispectral dataset was collected to examine its suitability for study of paintings of Goncharova and Larionov. As it did not offer information significantly different or superior to that derived by the SWIR imaging, this has not been otherwise reproduced or further analysed here but is available for extramural studies in the future.

subsequently quite brittle. Cracking of the thicker paint layers is obvious, and some areas have been somewhat abraded and slightly soiled.

B.3 Imaging

Each form of imaging offers different types of insight into the various material aspects of the painting. The most relevant are introduced, in brief, here.

B.3.i Photography with ultraviolet illumination

Excitation by ultraviolet (UV) light can induce luminescence⁶ in some materials, commonly seen as a weak re-emission of light in the visible region. Many natural varnishes have this property, emitting a characteristic weak greenish luminescence. While some pigments (notably zinc white and certain 'lake' pigments) are also active in this way, paints otherwise often do not luminesce. Because of the luminescence of varnishes, which are typically applied as a continuous coating across the surface of a painting, this can provide a means of determining if any disturbance has occurred, such as partial cleaning of the surface or addition of later restoration, where the changes show in contrast to the luminescent areas. Consequently, UV light is commonly used to reveal the presence of retouching. When paintings are not varnished, as is the case here, differences between the colour of the luminescence of the different paints and any added retouching paints can also indicate later stages of intervention (as here; **Protocol 3.2** and **Plate 2**).

In the UV image of this work, retouching is not readily distinguished. However, certain of the original paints exhibit distinct luminescence, notably, the yellow in the cheek and eyebrow of the proper left side of the face (yellow), the red of the top of the ear (orange red) and certain areas of blue. The white of the ground and the paint (lead white) shows as a clear white in the UV image.

The verso of the canvas shows a particular purplish fluorescence under UV illumination; however, the purple regions of fluorescence cannot be directly related to any of the compositional features of the recto.

B.3.ii Surface conformation

Two techniques for examination of the surface structure of the painting were used: photography under oblique illumination (**Plate 3**) and 3D laser scanning (**Plate 4**). While the former may be the more familiar of the two as a physical examination technique, both essentially provide a means of elucidating paint texture and object deformations, either by recording shadowing, or through direct measurement of surface height. Of the two, 3D laser scanning offers important advantages in terms of being more replicable in the future (to

⁶ Commonly referred to as 'UV fluorescence', the word *luminescence* is used here as a broader term that may encompass not only fluorescence phenomena (prompt re-emission of light), but also phosphorescence (slow re-emission of light due to transition via forbidden quantum states). In both cases emission is typically at longer wavelengths than the excitation; here, the excitation is in the UV to blue part of the spectrum (hence 'UV'; in practice, so-called UV-A) and emission in the visible region.

support longer-term conservation assessments for example) and as a numerical dataset that can be studied visually and algorithmically for diagnostic features of technique. Imaging of the painting using oblique illumination, as well as 3D laser surface scanning (see **Protocol 3.3**), served to reveal two kinds of textural features that are particularly evident in this painting. The most visually dominant is the narrow, horizontal banding that is associated with some of the most thickly painted areas. Areas of thick deposits of paint have set up a disruption in the stress present in the canvas, and thus, concentrations of stress cracks are localised to such areas. A comparison between the 3D image and the X-ray (**Plate 10.a**) is instructive in this regard; the X-ray reveals, in areas that image as white (radio opaque) the heaviest build-up of paint, which are exactly the areas with stress crack that is captured in the surface scan. The horizontal orientation is likely related to the horizontal nature of the stress of the stretching of the canvas, which can be seen in the thread density map that was generated by analysis of the X-ray (**Plate 11.a**)

Impasto arising from the brushwork is indicative of a fluid application of paint, with distinct build-up along edges of colour areas. For example, the contours of the head and face are effectively outlined by soft ridges of paint, as are the creases of the trousers at waist level.

B.3.iii Short-wave infrared (SWIR)

The interest in technologies capable of imaging artworks past the red end of the visible spectrum, in the ‘near’ (‘NIR’) or short-wave (‘SWIR’) infrared regions, has primarily developed out of the long-standing application to reflectography, exploiting the phenomenon of variable transparency of paint films at different wavelengths to enable visualisation of features lying beneath the surface. Imaging of underdrawing has been a major contribution to the study of authorship in paintings, permitting a fuller comprehension of artists’ working practices and extending the evidence used in attribution questions. Practical experience (as well as theoretical consideration) has shown that deeper IR cameras can confer additional benefits in terms of penetration to underlying layers; consequently, a system capable of operating in the SWIR region was used here (see **Protocol 3.4**).

In the IR image (**Plates 7, 8**), no discrete underdrawing can be resolved. However, examination of the canvas under magnification reveals the clear presence of a powdery, black-grey material, which apparently relates to the process of setting out the composition (see **Plate 7**, with indications of observed passages of underdrawing). The reason for this lack of resolution lies in a number of factors, probably a combination of the thin distribution of the material and the IR blocking properties of the thick overlying layers of paint.

B.3.iv X-radiography and weave analysis

X-radiography shows internal structures in paintings because the transmitted X-rays are blocked to different degrees by virtue of the inherent absorption and thickness variations of the constituent materials. For example, pigments based on lead (such as ‘lead white’, as here) stop the passage of X-rays more effectively than materials based on organic compounds (such as carbon blacks or the binding medium of the paint), while a thicker application of a material will block more than a thinner one. This allows visualisation of sub-surface features, such as

abandoned or altered earlier phases (*pentimenti*), use of techniques such as superimposed forms as opposed to forms left in reserve, characteristic brushwork and so forth.

Here, the prepared surface of the canvas is both heavily covered by the application of paint while in other areas, large swaths are only thinly coated or left exposed (such as the man's shirt). Consequently, the X-ray (**Protocol 3.6; Plates 10**) reveals a very direct rendition of form, with thickly painted areas imaging brightly (where they block the passage of X-rays), with dark areas adjacent to many of these forms. The dark areas corresponding to the thinly primed areas of canvas that were left visible (that is, unpainted; these are more X-ray transparent than heavily worked regions). Thus, while the Man's proper right arm shows as bright white, as it largely blocks the passage of the X-rays, the proper left side shows very darkly as it is only thinly painted.

Infilling of the interstices of the threads comprising the canvas support with the priming (ground) and paint also allows the canvas weave to be visualised in the X-ray (without the presence of the paint and lead containing ground, the carbon-based canvas would not be resolved by the X-ray). Even if a painting is lined, making direct access to the original canvas difficult or impossible, X-ray images can consequently permit the primary weave structure to be examined in detail. A common characterisation of canvases (apart from weave type) cited in the study of paintings is the 'thread count', or number of threads per unit in warp and weft directions. Conventionally determined by hand-measuring a number of representative areas, this is now done by applying an image processing algorithm to the entire X-ray image, which has the benefit of providing both greatly enhanced determination of thread counts as well as density and thread orientation information across the whole painting (see **Protocol 3.7; Plates 11.a-d**).

The thread count on this work was determined 16.4 threads per centimetre in the horizontal direction and 19.5 in the vertical. The well-distributed and even cusping distortion around the side edges of the canvas suggests that the painting retains its original format (**Plate 11.a**).

C. Sampling and analysis

C.1 Introduction

Samples were taken of the support, ground preparation, paint and varnish layers of the work for analysis by different means in order to determine the range of materials (canvas, pigments, binders and coatings) used in the painting, the nature of the preparation layer and the sequence of layering employed in building up the painting.

To this end, a series of 14 locations selected over a representative range of the painting were micro-sampled for identification of the pigments (**Table App.2.i, Plate 15**), with five micro-samples of paint taken for analysis of the binding media (**Tables App.2.ii-2.iv**). Two further samples were taken for preparation as cross-sections to study the layering in the selected areas, with the aim of elucidating the development of the painting (**Plates 16-20**). Finally, canvas threads were taken for fibre identification and radiocarbon dating (**Tables App.2.v and Tables App.2.vi**).

Micro-samples for analysis were taken from locations that were adjudged to be original (that is, were clearly contiguous with those below and adjacent to them, and not retouching or repair). Locations were also further selected to represent as wide a range of the colours – and therefore probably pigments and media – as possible. Thus, the materials identified and discussed below therefore represent, as far as can be determined, the full extent of the original palette used by the artist.

The micro-samples taken for pigment characterisation were subjected to systematic analysis by polarised light microscopy (PLM) combined with UV-visible-near infrared micro-spectrophotometry, scanning electron microscopy-energy dispersive X-ray spectrometry (SEM-EDX), Raman microscopy and some Fourier Transform Infrared Spectroscopy-Attenuated Total Reflectance (FTIR; **App.2.i**).

Organic components were identified by FTIR (**App.2.ii, Protocol 2.4.1**) and subsequently by Gas Chromatography-Mass Spectrometry (GCMS; **App.2.iii, Protocol 2.5**) and by staining of cross-sections with Sypro Ruby© (**App.2.iv, Protocol 2.6**).

All of the analytical techniques applied are standard methods within the field, capable of allowing the kinds of differentiation required for this type of work. Comparison was also made between samples from the painting and examples of similar pigments from a large collection of reference standards previously analysed by multiple means⁷. Certain differentiations cannot necessarily be made from this range of techniques, although for present purposes the level of discrimination is thought to be largely or wholly sufficient. All materials were generally identified through a combination of the techniques applied; however, certain key diagnostic features were specifically determined through one or other method.

C.2 Support

The canvas was identified as being based on linen (*Linum usitatissimum* L.) in the horizontal direction with a thread count of 16.4 threads per cm, and cotton (*Gossypium* spp.) in the vertical direction with a thread count of 19.5 threads per cm (that is, in alternate weave directions; **Plate 11, Protocol 3.7, App.2.v, Protocol 2.7**).

C.3 Radiocarbon dating

Radiocarbon dating was applied to fibres from the canvas support (**App.2.vi, Protocol 2.8**).

The radiocarbon date was determined as 121±23 years before present. After calibration, this yielded a date distribution for which the most relevant period for the origin of the canvas lies 1903-1939 at

⁷ The pigment reference collection belongs to the Pigmentum Project (see: <http://pigmentum.org>) and runs to around 3500 samples of both historical and modern origin. Analysis of this collection includes PLM and SEM-EDX as well as other techniques such as X-ray diffraction and Raman microscopy. Access to this research collection is gratefully acknowledged. Reference to specific specimens in the text of this report is to the Pigmentum collection number [Pxxxx]. An organic binding media reference collection is also held by AA&R; samples in this set are cited as [AARxxx].

the 95.4% probability level, pre-dating the so-called ‘bomb-pulse’ period that begins in the mid-1950s.

C.4 Ground

The ground (Sample [12]) was found to be composed primarily of a lead carbonate hydroxide type white (**Table App.2.i**) low levels of aluminium detected may indicate the presence of another phase such as aluminium oxide and/or hydroxide, although this was not otherwise confirmed. The ground is bound in a drying oil (**Table App.2.ii**). Protein detected in association with this layer by FTIR and a weakly positive result for SYPRO[®] Ruby staining is likely to be related to a minor protein component in the ground layer (**Table App.2.iv, Plate 20**). However, further characterisation, such as to demonstrate the use of a mixed medium with casein, was not pursued⁸.

C.5 Underdrawing

The underdrawing (though not captured in IR imaging due to its dispersed nature) was noted in various areas of the painting, where the ground is left exposed. Fragments occurring in the cross-section (Sample [16], **Plate 19**) are thought to be charcoal.

C.6 Paint layers: Pigments

The following primary pigments (**Tables App.2.1, App.2.2**) were identified:

- Lead carbonate hydroxide (‘lead white’)
- Cadmium sulfide (‘cadmium yellow’)
- Lead chromate (‘chrome yellow’)
- Zinc chromate yellow
- Earth pigments, red and yellow tones, containing hematite and goethite
- Mercury(II) sulfide (‘vermilion’)
- Lead(II, IV) oxide (‘red lead’)
- An organic red pigment on an aluminium phosphate sulfate substrate
- Ultramarine violet
- Manganese phosphate (‘manganese violet’)
- Iron hexacyanoferrate(II) (‘Prussian blue’)
- Ultramarine blue
- Chromium oxide hydrate with chromium borate (‘viridian’ green)
- Copper acetate arsenite (‘emerald green’)
- A bone coke (‘bone’ or ‘ivory’ black)

In addition, a range of white and colourless additives were found in combination with other colours, added in commercial preparations, including:

⁸ If significant amounts of casein were present, then phosphorus would probably have been detected by EDX.



- Zinc oxide ('zinc white')
- Barium sulfate
- An aluminosilicate clay mineral, kaolinite type

C.7 Paint layers: Binding media

All samples, including both ground and paint layers, indicated the presence of a drying oil (**Tables App.2.ii and 2.iii**); the binding medium of two paint samples was analysed (**App.2.iii**) and found to be consistent with walnut oil, or, with a mixture of linseed and poppy oil. However, the presence of protein was also noted in the paint to a limited degree (**Table App.2.iii, Table App.2.iv, Plate 20**).

Additionally, staining of a cross-section of sample [17] with SYPRO[®] Ruby indicated that the paint may contain a small amount of protein (**Table App.2.iv, Plate 20**).

FTIR also indicated the presence of metal soaps, probably of lead and zinc, assumed to be reaction products between pigments and binding medium. A soap in Sample [5], for which the primary pigment present is copper acetate arsenite, may be an organo-copper complex.

C.8 Stratigraphy

The preparation of cross-sections allowed for examination of the overall stratigraphy and composition of the priming and paint layers.

In Sample [15], a reddish-brown area of paint from the background along the lower edge (**Plates 15-17**) a thick layer of paint worked wet on wet is visible. White ground layer covered with a thick red-brown layer containing large red and colourless particles, and a few black particles. A yellow-orange paint is partially mixed in to the top part of this layer.

In Sample [16] a blue area of paint from the upper left edge (**Plates 15, 18-20**) a similar phenomenon – a thick layer of paint with a changing, stratified aspect – is present, again suggesting a painter working wet-in-wet with paint tones not thoroughly mixed to a consistent hue. Lowermost, the thick white ground may be seen, which is covered by a thin pale brown layer containing red, black and green particles, including one very large black splinter (relating to the underdrawing). This is followed by a very thick, striated overall paint layer, applied wet-in-wet with no clear boundaries. The lower portion is pale blue including some black and red particles. Halfway up is a green-blue band including a larger proportion of yellow particles, and the upper regions are darker blue, also including yellow, red and black particles. This may represent multiple applications of paint, or it may represent a loaded brush with many colours present – the lack of clear layer boundaries makes it difficult to say for sure what working process is responsible for the aspect of the paint.

D. Discussion of the findings

D.1 Support, ground and preparatory work

D.1.i The support

The painting has been executed on a plain-weave canvas of cotton and linen (a ‘union’ fabric), apparently spun with a z-twist in both cases. As no selvages are preserved, it is not clear which direction is warp and which is weft, although by convention the finer weave count direction is considered the warp. The cotton threads are aligned in the vertical direction with a thread count of 19.5 threads per cm, the linen threads in the horizontal direction with a thread count of 16.4 threads per cm canvas (**Plates 11, 12**); thus, the vertical cotton threads are to be considered the warp direction.

The canvas is of a medium weight, with relatively small interstices found between the threads. The canvas weave also exhibits relative uniformity, with few slubby or knotted threads.

The canvas is unlined, so the verso is fully visible (**Plates 5, 6**). It is affixed to a later, non-original, stretcher, primarily by means of round-headed tacks and by staples, that for the most part avoid the original tacking points, which are generally highly damaged by earlier metal corrosion (**Plates 12.b, 12.c**). The tacking margins may be seen to extend around the 2 cm thickness of the stretcher.

The stretcher appears to be of the same outer dimensions as the original version (80 x 95.5 cm) though the original bars may have been somewhat narrower than those present (bars now c. 5.5-.8 cm in width), as no noticeable change in dimensions of the painting may be discerned and no cracking associated with an earlier stretcher bar of different dimensions was observed. This is confirmed by the even cusping features found around the edges of the canvas (**Plate 11.a**). The inscriptions and labels present on the verso of the stretcher would seem to date to after the painter’s death⁹. Those on the verso of the canvas are described in more detail in the condition report prepared by Verena Franken¹⁰.

The use of union¹¹ fabrics based on cotton and linen appear to have come into use for French artists in the 19th century, increasing in popularity in the early 20th, although precise data is difficult to assemble. Callen for example has pointed out the lack of clear evidence on when a canvas contains fibre-types other than linen¹², although Vanderlip de Carbonnel states that she found cotton in use only from the very end of the 19th century, noting that ‘Cotton is first

⁹ These are described in more detail in V. Franken, *AAR0955.A 1483 Conservation Report* (2017b).

¹⁰ *Ibid.*

¹¹ Union fabrics have warp and weft of different fibre type, commonly a cotton warp combined with linen (as here), as well as wool, silk or synthetic fibres. The cotton warp would provide strength while being protected and showing the properties of the weft fibre on the surface. See for example: Denny, G.G. *Fabrics and how to Know Them: Definitions of Fabrics, Practical Textile Tests, Classification of Fabrics*, J.B. Lippincott Company: Philadelphia (1928) p. 121.

¹² Callen, A., *The Art of Impressionism. Painting technique & the making of modernity*, Yale University Press: New Haven and London (2000) pp. 30-31.

timidly introduced by being woven with linen [...] Then, at the beginning of the 20th century when the price difference between linen and cotton became considerable, all-cotton painting canvases appear¹³.

D.1.ii Priming

The canvas has been primed with a white ground layer composed of lead carbonate type white bound in oil. This appears to have been applied to the stretched canvas by hand, as it conforms to the painting surface but does not extend more than a small amount over the tacking margins (**Plate 12**). Its application is thin, and it was likely to have been applied in a rather liquid state; it has penetrated through the canvas to the verso, although the weave is not exceptionally open (**Plate 12.a**). There is no obvious sign of the use of an aqueous glue-based sealing layer (which would be applied before the white ground to reduce the absorbency of the canvas) noted on the verso, such as evidence of a glossy material. However, the possible presence of protein as noted in staining tests undertaken on a cross-section (**Plate 20**) suggests that perhaps a very thin layer (largely absorbed by the fibres and not obviously visible) was indeed used (**Table App.2.iii**, **Table App.2.iv**), though if so, it was clearly not applied in sufficient quantity to fully penetrate the canvas.

Both aspect of the canvas and the use of a thin, hand-applied priming might be seen in the context of an artist interested in working on a textured ground, and/or, an artist wanting to save money on supplies. Observed under the microscope, the priming is seen to have quite a ‘furry’ surface, given the thinness of the application (**Plates 13.a, 13.b**) though from a normal viewing range, it is the visibility of the canvas structure that dominates (**Plate 13.c**). The canvas is of a finer quality than many of the rough grade textiles used in some of both Goncharova and Larionov’s early works, is unusual in that it is made of mixed fibres (cotton in one direction of the weave, linen the other). Equally, as the ground is clearly applied by hand – this is not a factory prepared, ready to use painter’s canvas as was to become Goncharova’s preference after their move to Paris – less cost was likely incurred through the choice to mix the lead white and oil and applying the mixture as part of the process of creation. There is no evidence for the application of the ground onto the tacking edges; it extends only to the edges of the image plane. Given the use of wide brushes, evident brushstroke and little concern for smooth transitions and blending, this effect is well suited for the aesthetic of the work.

D.1.iii Underdrawing

The underdrawing (though not captured in IR imaging due to its dispersed nature) was noted in various areas of the painting, where the ground is left exposed (**Plates 7, 8**). Fragments occurring in the cross-section (Sample [16], **Plate 19**) are thought to be charcoal. In the detail taken from Sample [16] (**Plate 19**), in addition to the large, splinter like particle lying along the white ground, many smaller more rounded black particles may be seen in the paint above. These decrease in quantity towards the top of the sample. It is possible that these too

¹³ Vanderlip de Carbonnel, K., ‘A Study of French Painting Canvases’, *Journal of the American Institute for Conservation*, **20** #1 (1980) pp. 3-20. Information on the availability of these materials in Russia was not available to the authors; further information would be desirable.

represent the material of the underdrawing, pulled up into the paint layers as the brush passed over the friable, unbound and powdery material. Such underdrawings have been noted with increasing frequency in late 19th and early 20th century paintings; though they do not resolve well in IR imaging due to their diffuse nature (**Plates 7, 8**), they are clearly present as evidence to an early stage in the working process. It also seems that in this case, some faint drawn lines were applied during the painting process as they appear to sit over, not under, paint layers (**Plate 9**).

D.2 Paint, pigments and binding media

D.2.i General observations

The condition of the painting is generally quite good, although there is minor loss and flaking; the paint and ground are both of a rather matte, brittle aspect, and the paint, especially where thick, exhibits broad brittle crack formation. As noted above, although it is on a new stretcher, it retains its original dimensions and retains sufficient tension.

The painting is executed in a very sure and spontaneous manner after the forms were laid in with a charcoal underdrawing. The prepared surface of the canvas is alternately thickly covered by the application of paint, which extends to, and slightly over, the tacking margins, and as well as left exposed (such as in the area of the man's shirt). The extremes of thick paint and exposed areas are visible in the high contrast aspect of the X-ray (**Plate 10**).

D.2.ii Paint: pigment and binding medium

The painting displays a marked horizontal crack pattern in areas where the paint is thickly applied, which relates to the nature of the stresses in the canvas due to stretching (**Plate 11.a**). This is particularly visible in the 3D surface scan (**Plates 4**).

Observation of the verso of the canvas reveals some slight darkening of the threads, though this is not obviously related to penetration of oil from the recto, as the shapes do not correspond with the composition (**Plates 5, 6**). As noted above, penetration of the white ground through the canvas to the verso is evident, though again, not consistent or regular in form.

The palette used in this painting is quite extensive in the context of Larionov's work: four yellow tones, four red/orange tones, two purple tones occurred together in the same sample (Sample [2]), two blue tones and two green tones were noted. The pigments are generally quite finely ground; exceptions include the large black fragments pertaining to the charcoal underdrawing, and the somewhat larger particles of crimson lake (as seen in cross-section, Sample [15], **Plate 17**). The binding medium of two paint samples was analysed (**App.2.iii**) and found to be consistent with walnut oil, or, with a mixture of linseed and poppy oil. However, the presence of protein was also noted in the paint to a limited degree (**Table App.2.iii, Table App.2.iv, Plate 20**). It may be that the protein and oil emulsions were used, in part, throughout the painting to impart both impasto and a matte aspect.

The cross-sections prepared confirm the observations made on the surface, and with the various forms of imaging: the paint was worked freely and directly (**Plates 16-20**). Within a thick layer many soft transitions of colour can be seen, suggesting that the artist was mixing paints on the palette and working extensively wet-in-wet. This direct application has led to quite thin passages where the canvas weave and lumpy texture of the ground remain fully visible, and others where it is fully obliterated by a heavy build-up of impasto. Some of the fields of colour are delineated from one another by dark contours, which were primarily added as the final program of working.

No evidence for complex layering was seen; areas are worked quite directly, with mixing both on the palette, and wet-in-wet directly on the canvas. The colours are bright and intense, the paint strongly opaque and used quite thickly as well as spread thinly in other passages. No use of transparent glazes was observed, though a transparent crimson lake was employed (recognisable in UV for its bright orange luminescence, **Plate 2**). Where this tone has been used, it is employed the same manner as the other paints, not as a subtle modifying layer (**Plate 14.c**). The colours remain intense, though the surface aspect is quite matte. The painting does not show evidence of having been varnished, in keeping with the artist's preference for a brightly coloured, rough, matt finish.

The textured aspect of the painting is created both through the artist's use of impasto (**Plates 3, 4**) but also heightened by alterations in the paint film that have taken place; the formation of metal soaps – lead, zinc and copper based, in different areas of the painting - was noted in the FTIR analysis (**Table App.2.ii**), which likely corresponds to the obvious rounded protrusions seen in many areas of the work (**Plate 14**). This is related to the use of oil in the binding medium, which reacts with metals in certain of the pigments to form the aforementioned metal soaps.

D.2.iv Materials analysis and implications for dating

The painting has been dated to 1910. Of the data collected, nothing came to light that would speak against that particular dating, although equally, it would allow for a somewhat earlier or later ordering as well.

The radiocarbon measurement of the canvas gave an origin for it between 1903-39 at the 95.4% probability level, though pre-dating the so-called 'bomb-pulse' period that begins in the mid-1950s. In addition to this a period of 3-5 years typically needs to be allowed for processing into canvas and use by the artist, making a date of 1910 reasonable, though suggesting a later dating possible also. An earlier calibrated date range of 1802-95 appears unlikely for similar reasons (that is, including a processing allowance does not make it plausible), though not wholly impossible if the canvas had been kept for longer than normal. As noted above, the cotton-linen union fabric, although unusual in that it has not often been documented in use, would be plausible in this period.

The materials otherwise identified in the painting are compatible with the supposed date (although they were also in use somewhat earlier and continued in use for some decades after that time).

The findings generally agree well with the data collected in the study of 45 paintings by Goncharova and Larionov in the collection of the Musée national d'art moderne, Paris¹⁴. Though some of the technical aspects noted here were not identified in that study, they are still highly plausible for the period in question¹⁵.

Other technical characteristics arising from the larger review of the works of Goncharova and Larionov may also contribute to a fuller understanding of the relative dating of this painting in the future.

E. Conclusions

The examination of the painting revealed a work that was created with great spontaneity, first with an initial lay in in a powdery drawing medium (likely charcoal) followed by application of bright colour fields composed from a rich palette of materials. The fact that the ground is hand applied is characteristic of Larionov's practice, as is the free working of colours, often wet-in-wet. In comparison, the use of a lead white ground and a canvas of mixed fibre composition (cotton and linen) are unusual for what is known of Larionov's choice of materials, but not (in the case of the lead white ground) unprecedented. The date of the work given, 1910, is plausible in light of the findings.

¹⁴ The ground presents the single exception, in that only grounds based on zinc white were noted in those examples prepared by the artists themselves. Rioux, Aitken and Duval (1998) *op. cit.* p. 18.

¹⁵ The Paris research (*ibid.*) did not find any examples of grounds composed of materials other than zinc white (here lead white), or canvases composed of fibres other than pure linen (here linen and cotton). However, these are wholly period appropriate. Equally, the palette here is quite rich in the variety of pigments used.



F. Acknowledgements

Art Analysis & Research would like to thank the following people for their contributions:

Museum Ludwig

Dr Yilmaz Dzewior	Director, Museum Ludwig	
Rita Kestring	Deputy Director, Museum Ludwig	
Petra Mandt	Deputy Head of Conservation, Museum Ludwig	Project coordinator Paintings conservator

Project Team, AA&R

Dr Jilleen Nadolny	Principal Investigator	Project management
Dr Nicholas Eastaugh	Chief Scientist	Materials and data analysis
Bhavini Vaghji	Senior Scientist	Materials analysis
Francis Eastaugh	Senior Imaging Engineer	Scientific imaging processing
Dr Joanna Russell	Scientist	Materials analysis

Project Subcontractors

Verena Franken	Freelance paintings conservator, Cologne, Germany	Project coordinator, examination, documentation and archival research
Patrick Schwarz	Rheinisches Bildarchiv Köln, Cologne, Germany	Photographic documentation
Prof. Hans Portsteffen, Andreas Krupa	Department of Conservation, Cologne University of Applied Sciences, Germany	Capture of X-ray data
Xavier Aure-Calvet	Freelance imaging specialist, Bristol, UK	3D imaging capture and post processing
Prof Haida Liang and team	Nottingham Trent University, UK	Hyperspectral imaging
Dr Irka Hadjas and team	ETH/ Swiss Federal Institute of Technology, Zurich, Switzerland	Radiocarbon analysis

We would also like to extend our sincere thanks to the Peter and Irene Ludwig Foundation and to the RARP donors and to its board of trustees, without whose generosity and vision this project would not have been possible.

G. Appendices

Standard protocols used by AA&R in the preparation of this report for sampling, materials analysis and imaging are listed in each subsection below and detailed in the appendices to the global summary report.

App.1 Sampling and sample preparation

Protocols:

[P.1.1] Sampling

[P.1.2] Cross-sectional analysis

App.1.i. Sampling

Table App.1.i Samples taken for analysis				
#	Colour	Description	Location ¹⁶	Analysis
1		Bright Blue	342/949	PLM, SEM-EDX, Raman
2		Purple	295/913	PLM, SEM-EDX, Raman
3		Orange	292/913	PLM, SEM-EDX, Raman
4		Red	310/899	PLM, SEM-EDX, Raman
5		Green	316/902	PLM, SEM-EDX, Raman, FTIR, GC-MS
6		Yellow	304/845	PLM, SEM-EDX, Raman
7		Dark Transparent Red	449/921	PLM, SEM-EDX, Raman
8		Light Brown	326/1011	PLM, SEM-EDX, Raman, FTIR
9		Reddish Brown	357/989	PLM, SEM-EDX, Raman, FTIR
10		Black	358/1042	PLM, SEM-EDX, Raman

¹⁶ The x/y coordinates in this column are given in millimetres from the left-hand and lower edges of the painting.

Table App.1.i Samples taken for analysis				
#	Colour	Description	Location ¹⁶	Analysis
11		White	860/322	PLM, SEM-EDX, Raman, FTIR, GC-MS
12		White Ground	690/377	PLM, SEM-EDX, Raman, FTIR
13		Green	225/616	PLM, SEM-EDX, Raman, FTIR
14		Black Underdrawing	220/410	PLM, SEM-EDX, Raman
15		Brown	1/88	CSA
16		Blue	1/1036	CSA, SYPRO [®] Ruby Staining
17		Fibres, canvas	0/0	PLM, FTIR, C14
18		Green (as 5)	316/902	GC-MS
19		White	310/250	GC-MS

App.1.ii Cross-sectional analysis

Results are shown in **App.5, Plates 16-20**.

App.2 Materials analysis summary results

Protocols:

- [P.2.1] Polarised light microscopy (PLM)
- [P.2.2] Scanning electron microscopy-energy dispersive X-ray spectrometry (SEM-EDX)
- [P.2.3] Raman microscopy
- [P.2.4.1] Fourier Transform Infrared Spectroscopy-Attenuated Total Reflectance (FTIR-ATR)
- [P.2.5] Gas Chromatography-Mass Spectrometry (GCMS)
- [P.2.6] Protein staining with Sypro Ruby[®]
- [P.2.7] Fibre Identification
- [P.2.8] Radiocarbon dating

App.2.i SEM-EDX, Raman microscopy and PLM analysis

#	Colour	SEM-EDX (elements)			Raman Microscopy (peaks, cm ⁻¹)	Identification
		Major	Minor	Trace		
1	Bright blue	Si	Na, Al, S	<i>Mg, P, K, Ca, Cr, Fe, Zn, Hg, Pb</i>	585 (vw, sh), 548 (w), 256 (vw)	Ultramarine (main) Mercury sulfide (trace) Zinc oxide (trace)
2	Purple	-	Al, Si, P, S	<i>Na, Mg, K, Ca, Ti, Mn, Ba</i>	889 (vw), 611 (vw), 568 (vw), 547 (vw), 368 (vw), 298 (vw), 254 (vw), 218 (vw)	Ultramarine violet [P0100] Manganese phosphate [P1351]
3	Orange	Pb	S, Ba	<i>Al, Si, Zn</i>	1050 (vw), 987 (vw), 549 (w), 455 (vw), 390 (w), 313 (vw), 224 (vw), 151 (w), 121 (vs)	Red lead [P0071] Lead carbonate type white Barium sulfate
					987 (vw), 842 (vw), 549 (w), 454 (vw), 390 (w), 361 (vw), 314 (vw), 231 (vw, sh), 225 (vw), 151 (w), 121 (vs)	Red lead [P0071] Lead chromate (trace) ¹⁷ Barium sulfate Zinc oxide (trace)
4	Red	S	Al, Hg	<i>Mg, Ca, Ba</i>	343 (w), 284 (vw), 254 (vs), 108 (vw)	Mercury sulfide [P0010]
5	Green	As	Cu	<i>Al, Si, S</i>	368 (vw), 247 (vw), 218 (vw), 153 (vw), 121 (vw)	Copper acetate arsenite [P1302]
6	Yellow ¹⁸	Cr, Pb	Al	<i>Mg, Si, P, S, Ca, Fe, As</i>	969 (vw), 840 (vs), 401 (w), 377 (w), 359 (s), 338 (w), 327 (w), 180 (vw), 136 (w)	Lead chromate yellow [P2238] (main) Iron containing earth pigments (trace)
7	Dark transparent red	Al, P	S	<i>Na, Mg, Si, Ba, Hg</i>	1293 (vw), 343 (w), 283 (vw), 253 (s)	Mercury sulfide (trace) Organic pigment on Al/P/S substrate (main)
8	Light brown	Si	Al, Fe, Zn	<i>S, K, Ca, Cr, As, Ba, Hg, Pb</i>	840 (vw), 391 (vw), 359 (vw), 293 (vw), 255 (vw), 226 (vw)	Hematite Goethite Mercury sulfide (trace) Lead chromate (trace) Zinc oxide
9	Reddish brown	Fe	Si	<i>Al, P, S, K, Ca, As</i>	405 (vw), 292 (vw), 222 (vw)	Hematite

¹⁷ Chromium was not identified in the SEM-EDX analysis.

¹⁸ A reddish brown pigment was observed.

Table App.2.i Analytical results SEM-EDX, Raman Microscopy and PLM

#	Colour	SEM-EDX (elements)			Raman Microscopy (peaks, cm ⁻¹)	Identification
		Major	Minor	Trace		
10	Black	-	P, Ca	<i>Na, Mg, Al, Si, S, Cl, K, Cr, Fe, Cu, Pb</i>	1587 (w, br), 1300 (w, br)	Carbon-based black (bone or ivory black)
11	White	Pb	-	<i>Al, Si</i>	1362 (vw, br), 1049 (m), 679 (vw), 413 (vw, br), 322 (vw), 108 (vs)	Lead carbonate hydroxide [P0864]
12	White ground	Pb	Al ¹⁹	-	1364 (vw, br), 1050 (w), 679 (vw), 413 (vw, br), 123 (vw, sh), 109 (s)	Lead carbonate hydroxide [P0864]
13	Green	Cr	S, Ba	<i>Al, Si, K, Ca, Zn, As, Sr, Pb</i>	-	Chromium oxide green (main) Barium sulfate (minor) Zinc oxide (trace)
14	Black	-	S, Ca, Zn, Pb	<i>Al, Si, P, K, Cr, Fe, Cd</i>	1574 (vw, br), 1298 (vw, br)	Carbon-based black Cadmium sulfide Chromium oxide green Zinc oxide Lead carbonate type white

App.2.ii Fourier Transform Infrared Spectroscopy-Attenuated Total Reflectance (FTIR-ATR)

Table App.2.ii Summary results from FTIR

#	Colour	FTIR (peaks, cm ⁻¹)	Identification
5	Green	3257 (vw, br), 2920 (w), 2851 (vw), 1732 (vw, sh), 1707 (m), 1615 (vw), 1554 (s), 1448 (s), 1416 (w), 1301 (vw), 1244 (vw), 1173 (vw), 1089 (vw), 1025 (vw), 814 (m), 756 (s), 688 (vw), 631 (s)	Copper acetate arsenite [P1302] Oil Metal soap formation, presumably copper-based ²⁰
8	Light brown	3698 (vw), 3187 (vw, br), 2954 (vw, sh), 2916 (s), 2849 (m), 1733 (m), 1714 (w), 1623 (vw), 1593 (vw), 1547 (s), 1529 (s), 1456 (m), 1408 (vw, sh), 1398 (m), 1319 (vw), 1165 (w), 1089 (m), 1027 (m), 1005 (s), 910 (w), 876 (vw), 795 (w), 779 (vw), 745 (w), 719 (vw), 694 (vw), 683 (vw)	Aluminium silicate clay mineral, kaolinite type Goethite Oil Metal soap formation, zinc-based ²¹ Metal soap formation

¹⁹ Phase unidentified, but perhaps an aluminium hydroxide given absence of other associated elements. Level is at about 1% of total.

²⁰ It is assumed that the metal soap present in the sample is copper-based since copper acetate arsenite was the main component identified in the sample.

Table App.2.ii Summary results from FTIR			
#	Colour	FTIR (peaks, cm⁻¹)	Identification
11	White	3534 (vw), 3278 (vw, br), 2921 (w), 2851 (vw), 1734 (w), 1717 (vw, sh), 1616 (vw), 1523 (w), 1387 (vs), 1354 (w, sh), 1168 (vw), 1090 (vw), 1043 (vw), 852 (vw), 767 (w), 756 (vw, sh), 706 (vw), 679 (vs)	Lead carbonate hydroxide Oil Metal soap formation, presumably lead-based
12	White ground	3537 (vw), 3283 (vw, br), 2919 (vw), 2849 (vw), 1739 (vw), 1647 (w), 1539 (vw), 1393 (vs), 1086 (vw), 1044 (w), 968 (vw), 864 (vw), 843 (vw), 766 (w), 680 (vs)	Lead carbonate hydroxide Protein Binding media component (type unidentified) ²²
13	Green	3441 (vw, sh), 3193 (w, br), 2954 (vw, sh), 2916 (m), 2849 (w), 2097 (vw), 1732 (w), 1712 (vw), 1614 (vw), 1592 (vw), 1539 (s), 1454 (s), 1418 (vw, sh), 1397 (vw), 1360 (w), 1283 (s), 1250 (m), 1172 (w), 1067 (s), 982 (vw), 946 (m), 876 (s), 797 (m), 719 (vw), 695 (vw), 679 (vw), 654 (vw, sh), 633 (vw, sh), 606 (w)	Chromium borate ²³ Prussian blue Zinc chromate [P2251] Barium sulfate Carbonate ²⁴ Oil ²⁵ Metal soap formation, zinc-based ²⁶

²¹ The peaks present in the sample spectrum matched the reference spectrum of zinc stearate, reference number AAR308. Zinc was identified in the SEM-EDX analysis.

²² The four peaks present are peaks assigned to the binding medium however from these four peaks it is unclear what the binding medium is as there are multiple binding media which show these mentioned peaks such as oils, alkyds and natural resins to name a few.

²³ The peaks assigned to chromium borate are present in the reference spectrum of chromium oxide hydrate, reference number P0092.

²⁴ It is not possible to say in which form the carbonate is since both lead carbonate type white and calcium carbonate show this peak. Other peaks which can be used to differentiate one from the other are absent.

²⁵ The characteristic peak of oil occurring at around 1160 cm⁻¹ was not observed in the spectrum due to the presence of barium sulfate whose peaks were masking this characteristic peak of oil however it is assumed that oil is present due to the formation of metal soaps.

²⁶ The peaks present in the sample spectrum matched the reference spectrum of zinc stearate, reference number AAR308. Zinc was identified in the SEM-EDX analysis.



App.2.iii Gas Chromatography-Mass Spectrometry (GCMS) Analysis

Table App.2.iii Summary results from GCMS					
Sample #	Hexadecanoic acid, methyl ester (C ₁₇ H ₃₄ O ₂)		Octadecanoic acid, methyl ester (C ₁₉ H ₃₈ O ₂)		Ratio
	Retention time, mins	Peak area	Retention time, mins	Peak area	
J 18	25.650	3.761 x 10 ⁸	29.593	1.060 x 10 ⁸	P/S = 3.55
J 19	25.650	2.504 x 10 ⁹	29.586	7.844 x 10 ⁸	P/S = 3.19

The P/S value of Sample [18], green paint, was 3.55, consistent with **walnut oil** or a **mixture of linseed and poppy oil**.

The P/S value of Sample [19], white paint, was 3.19, consistent with **walnut oil** or a **mixture of linseed and poppy oil**.

App.2.iv SYPRO[®] Ruby protein staining

Table App.2.iv SYPRO [®] Ruby stain results for sample [16] ²⁷ .				
Layer	EDX	FTIR	SYPRO [®] Ruby stain	Interpretation
Ground	Pb Al	Protein	Patchy pink staining, stronger towards outer edges of sample. ²⁸	Protein in ground
Paint	-	[In other samples: oil clearly identified in green, light brown, white. Binder unidentified in yellow and red brown]	Pink stain has clearly been taken up by lighter blue paint. More difficult to tell in darker blue areas.	Protein in paint layers

²⁷ For the ground layer, EDX and FTIR data derives from separate analysis of another sample.

²⁸ The darker staining at the edges of the ground layer appears to correspond to areas at the periphery of the sample, rather than to a distinct layer at the base of the cross section. There is not sufficient evidence to identify this as a size layer.

App.2.v Canvas fibre identification

Table App.2.v Canvas fibre identification		
<i>Sample</i>	<i>Observations under PLM</i>	<i>Interpretation</i>
17 horizontal	Nodes across fibres, parallel extinction, S-twist. A few structures with low birefringence, some appearing as broadened ends of fibres (possibly degraded areas).	Bast fibre, probably linen (<i>Linum usitatissimum</i> L.)
17 vertical	Twisted ribbons, no clear extinction.	Cotton (<i>Gossypium</i> spp.)

App.2.vi Radiocarbon measurement

Radiocarbon dating is a method for determining age estimates of formerly living organic materials²⁹. Carbon has three naturally occurring isotopes, ¹²C, ¹³C and ¹⁴C. Both ¹²C and ¹³C are stable, but ¹⁴C decays by very weak beta decay to nitrogen (¹⁴N) with a half-life of approximately 5,730 years. While alive, organic materials continue to exchange carbon with the environment, such that they are in equilibrium. On death, the ¹⁴C component begins to decay, such that over time the relative amount decreases. Measuring the level of ¹⁴C remaining in the material then allows for a date to be estimated. This must be additionally calibrated against natural historical variation in relative ¹⁴C levels in the environment, for which there are accepted standard curves expressing the changes over time³⁰.

Prior to radiocarbon measurement, fibre identification was undertaken, and the canvas sample was pre-tested using FTIR to ascertain the presence of any contaminating material that could influence the outcome. As noted elsewhere, the fibre was identified as a bast type, probably linen (*Linum usitatissimum* L.), in the horizontal direction and cotton (*Gossypium* spp.) in the vertical direction. FTIR indicated the presence of calcium sulfate (gypsum type), and possibly an oil, in addition to the cellulose of the fibre³¹.

The canvas sample was then submitted to the Laboratory of Ion Beam Physics, ETHZ at the Swiss Federal Institute of Technology (*Eidgenössische Technische Hochschule Zürich*) for radiocarbon dating (see **Protocol 2.8**).

²⁹ Based on from the websites of the NDT Resource Center, <http://www.ndt-ed.org/EducationResources/CommunityCollege/Radiography/Physics/carbondating.htm> and the website of the Oxford Radiocarbon webinfo site: <http://c14.arch.ox.ac.uk/embed.php?File=webinfo.html>, both consulted on 3 February 2013.

³⁰ For example, that used here is one known as IntCal13.

³¹ Non-cellulosic materials are aimed to be removed by the sample pre-treatment process prior to the radiocarbon measurement.

Table App.2.vi.i Radiocarbon measurement										
Sample-Nr.	Sample Code	Material	C14 age BP	$\pm 1\sigma$	F14C	$\pm 1\sigma$	$\delta C13$ ‰	$\pm 1\sigma$	mg C	C/N
ETH-77075	AAR0955.J.17	Textile fibre	121	23	0.985	0.003	-20.4	1	0.9	262.4

The radiocarbon date was determined as 121 years b.p. ± 23 years. After calibration, this yielded a date distribution for which the most relevant period for the origin of the canvas lies 1903-1939 at the 95.4% probability level, pre-dating the so-called ‘bomb-pulse’ period that begins in the mid-1950s.

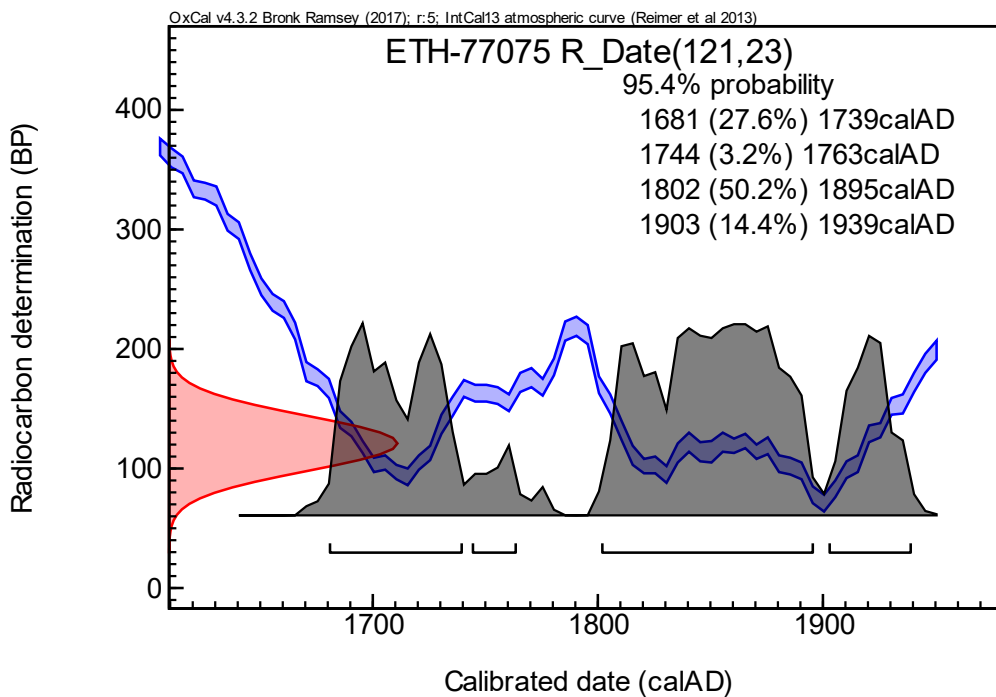


Figure App.2.vi.ii Radiocarbon determination.



App.3 Imaging methods

Protocols:

- [P.3.1] Photography with visible light
- [P.3.2] Photography with ultraviolet illumination
- [P.3.3] 3D laser surface mapping
- [P.3.4] SWIR infrared imaging (IR)
- [P.3.5] Multispectral visible-NIR imaging
- [P.3.6] X-radiography
- [P.3.7] Thread counting and weave analysis

App.4 Plates

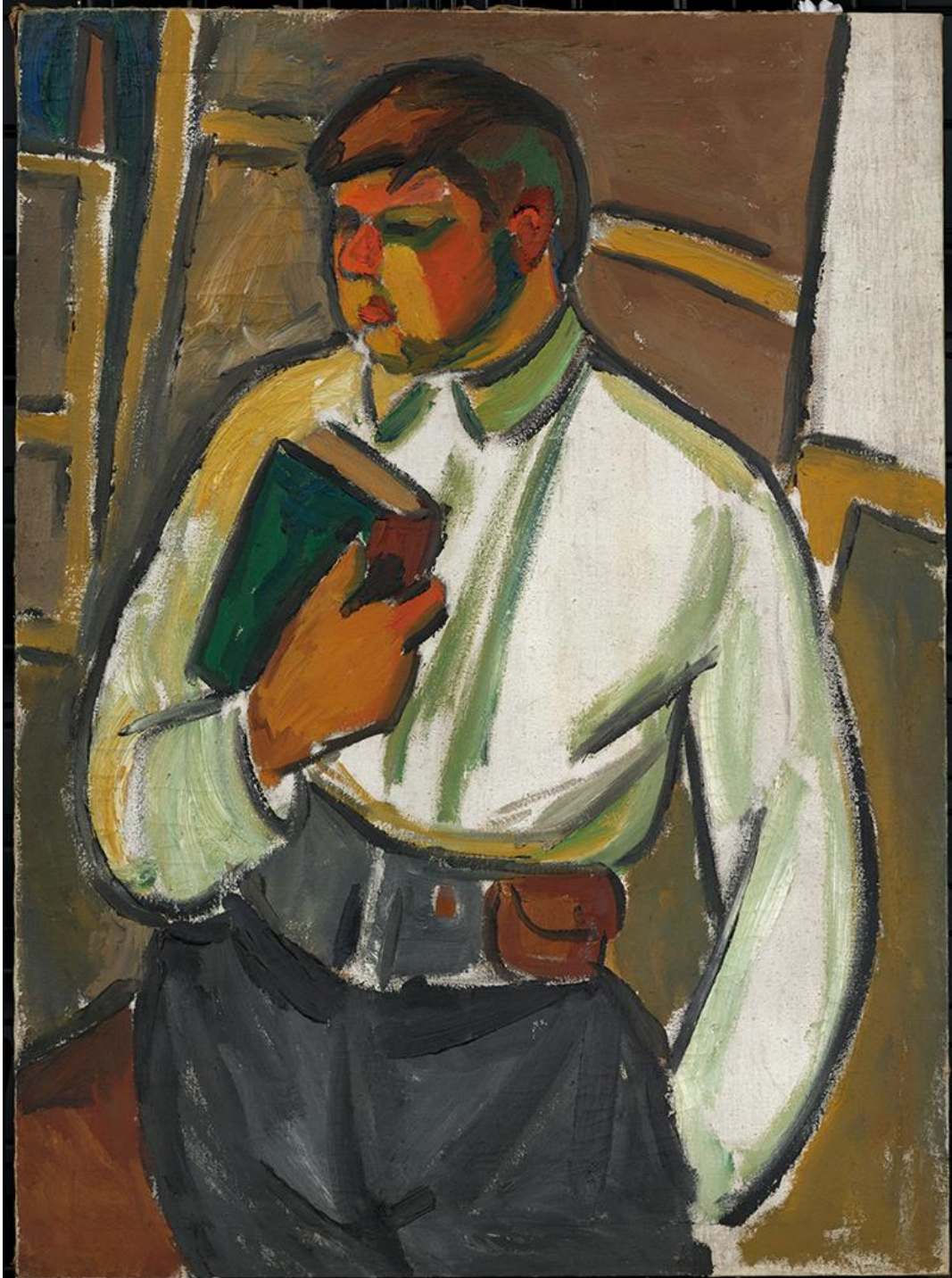


Plate 1. Mikhail Larionov, *Portrait of a Man (Anton Beswal)*, c. 1910, collection Museum Ludwig: Inv. Nr. ML 1306. **Recto, visible light.**

Rheinisches Bildarchiv Köln, Patrick Schwarz, rba_d050880_09, www.kulturelles-erbe-koeln.de/documents/obj/05020020



Plate 2. Mikhail Larionov, *Portrait of a Man (Anton Beswal)*, c. 1910, collection Museum Ludwig: Inv. Nr. ML 1306. **Recto, UV light.**

Rheinisches Bildarchiv Köln, Patrick Schwarz, rba_d050880_07, www.kulturelles-erbe-koeln.de/documents/obj/05020020

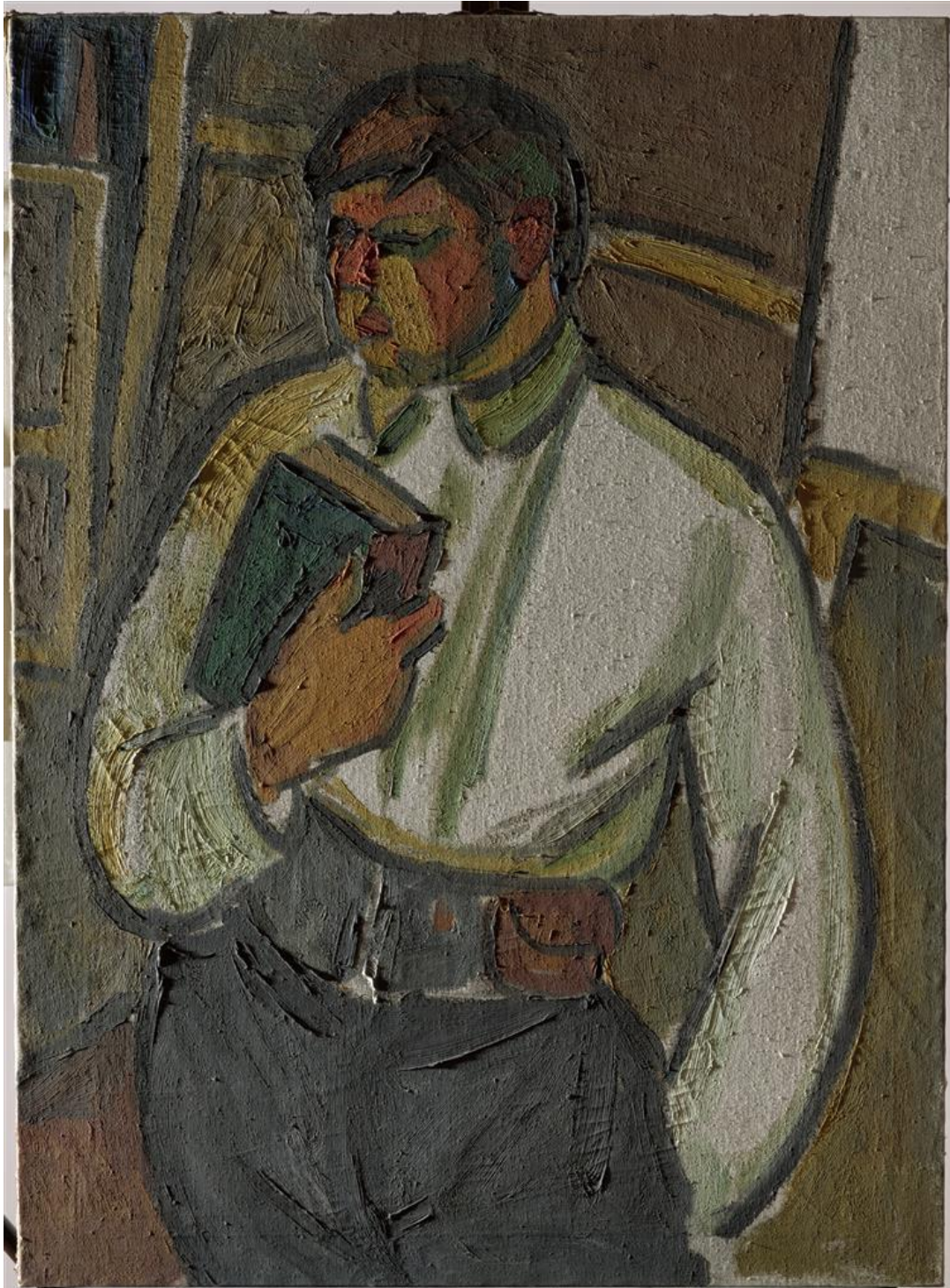


Plate 3. Mikhail Larionov, *Portrait of a Man (Anton Beswal)*, c. 1910, collection Museum Ludwig; Inv. Nr. ML 1306. **Recto, oblique illumination.**

Rheinisches Bildarchiv Köln, Patrick Schwarz, rba_d050880_04, www.kulturelles-erbe-koeln.de/documents/obj/05020020



Plate 4. Mikhail Larionov, *Portrait of a Man (Anton Beswal)*, c. 1910, collection Museum Ludwig: Inv. Nr. ML 1306. **Recto, 3D laser scan.**



Plate 5. Mikhail Larionov, *Portrait of a Man (Anton Beswal)*, c. 1910, collection Museum Ludwig: Inv. Nr. ML 1306. **Verso, visible light.**

Rheinisches Bildarchiv Köln, Patrick Schwarz, rba_d050880_02, www.kulturelles-erbe-koeln.de/documents/obj/05020020



Plate 6. Mikhail Larionov, *Portrait of a Man (Anton Beswal)*, c. 1910, collection Museum Ludwig: Inv. Nr. ML 1306. **Verso, UV light.**

Rheinisches Bildarchiv Köln, Patrick Schwarz, rba_d050880_08, www.kulturelles-erbe-koeln.de/documents/obj/05020020



Plate 7. Mikhail Larionov, *Portrait of a Man (Anton Beswal)*, c. 1910, collection Museum Ludwig: Inv. Nr. ML 1306. **Recto, SWIR image.**

Detail showing extent of underdrawing, in red, observed with the microscope.



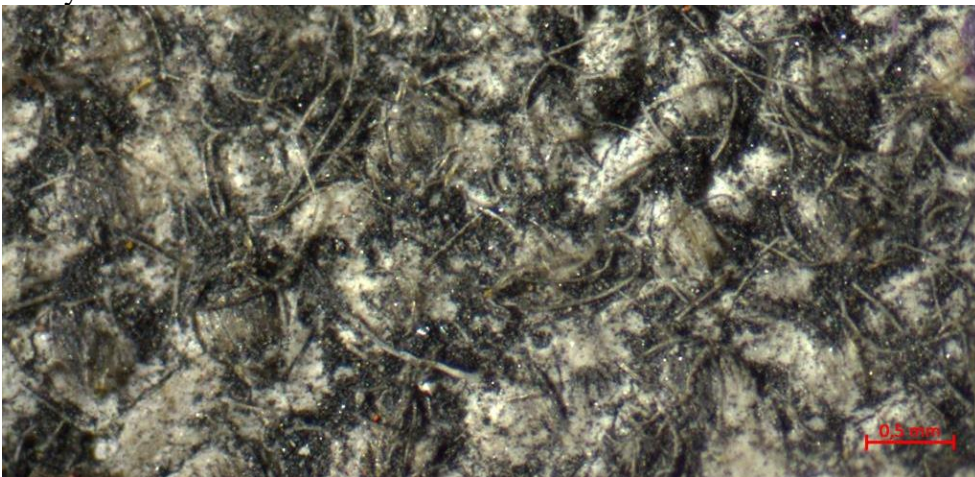
a.



b.

Plate 8. Detail of underdrawing, recto.

a.) SWIR (as plate 7), b.) visible light. Below, c.), microscope detail, black material between the eyebrows.



c.



a.

Plate 9. Recto, detail, drawing, upper proper left arm.

a.) SWIR image, upper proper left arm, below b.) visible light. The pale lines, left, may be seen to run over the green paint.



b.



Plate 10.a Mikhail Larionov, *Portrait of a Man (Anton Beswal)*, c. 1910, collection Museum Ludwig: Inv. Nr. ML 1306. **X-ray image.**

Plate 10.b The X-ray image before digital compensation for the stretcher bars.

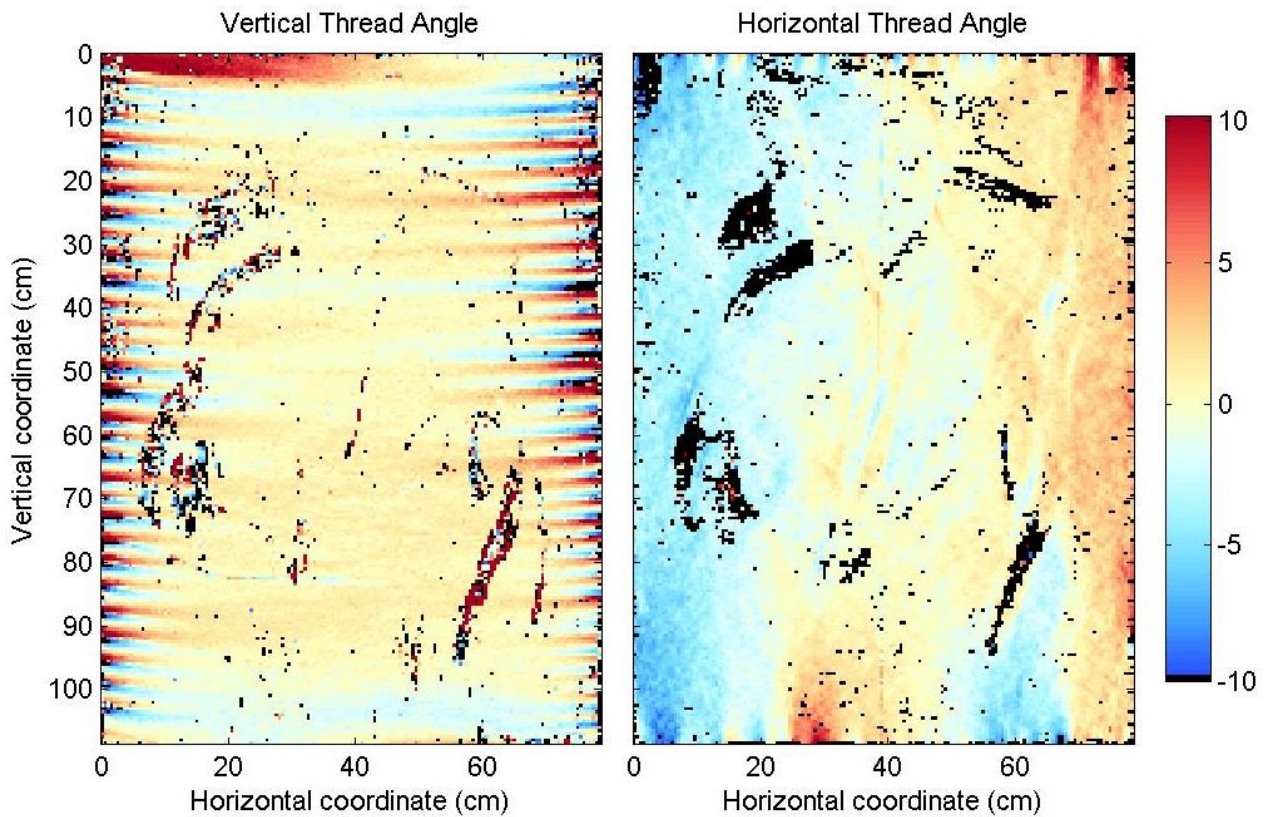


Plate 11.a Maps showing variation in canvas thread angle.

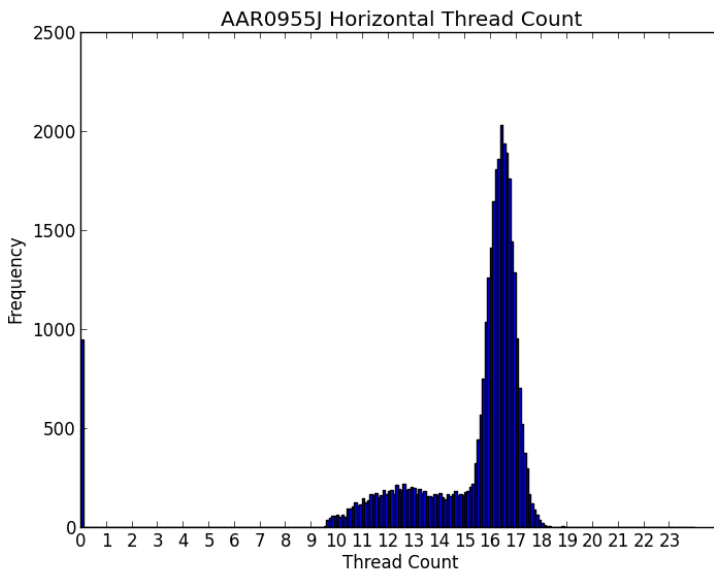


Plate 11.b Histogram of horizontal thread (in this case related to the warp) count readings.

Showing variation in thread count per centimetre.

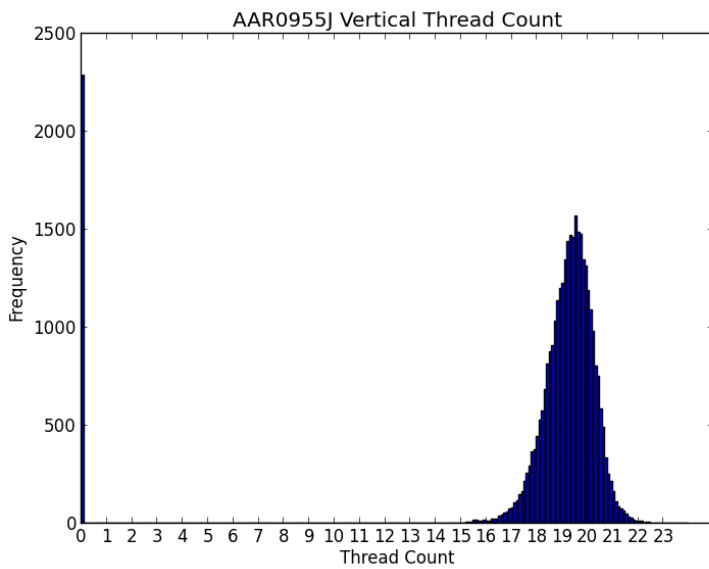


Plate 11.c Histogram of vertical thread count readings (in this case related to the weft).

Showing variation in thread count per centimetre.

Plate 11.d Table of thread count data (threads per centimetre)		
	Mean	Estimated thread count (mode)
Horizontal	15.55	16.4
Vertical	19.34	19.5



Plate 12.a Detail of canvas, verso.

The canvas is a thin, plain weave type, with the selvedge edge running vertically. The fibre type is apparently linen (*Linum usitatissimum* L.) in the horizontal direction and cotton (*Gossypium* spp.) in the vertical. The white priming may be seen to penetrate the canvas.



Plate 12.b Detail of canvas, right tacking margin, showing selvedge, right, along top edge.

The thin, white priming may be seen under the paint.



Plate 12.c Detail of canvas, right tacking margin, showing selvedge.



Plate 13.a Microscope detail of the lead white-based priming on the canvas, recto.

Shows the thin aspect of this layer, which allows the canvas fibres to remain distinct upon the surface.



Plate 13.b Detail of the black material that may form the laying in, or 'underdrawing'.

As Plate 8.



Plate 13.c Detail of the cusping of the exposed, primed canvas along the tacking margins.

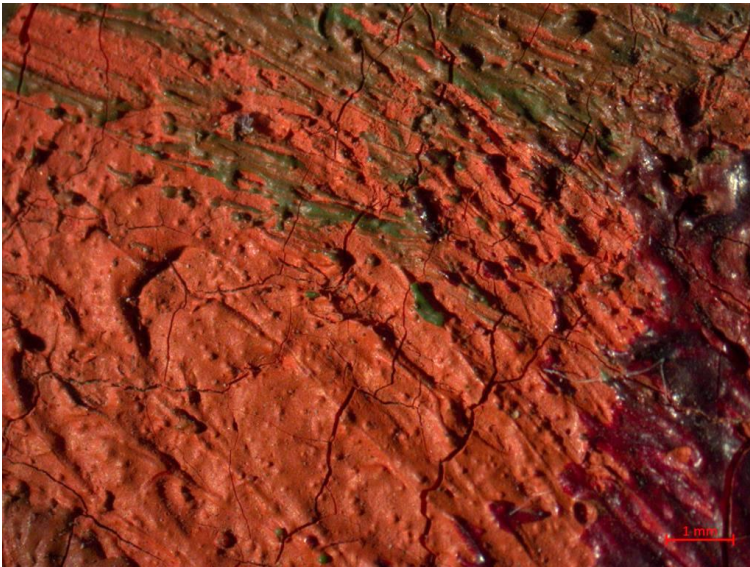


Plate 14.a Macro detail of the brittle cracking and granular nature of some of the painting's surface.



Plate 14.b Detail of protrusions from the underlying layer, projecting through the overlying brown.

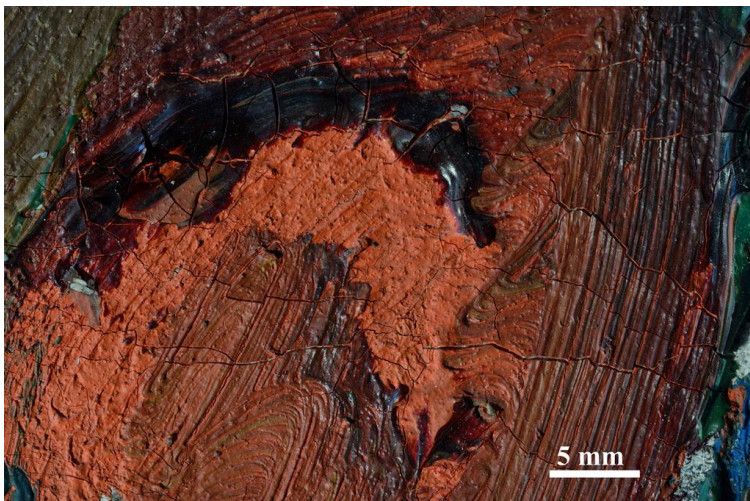


Plate 14.c Macro detail of the brittle cracking of the paint film.

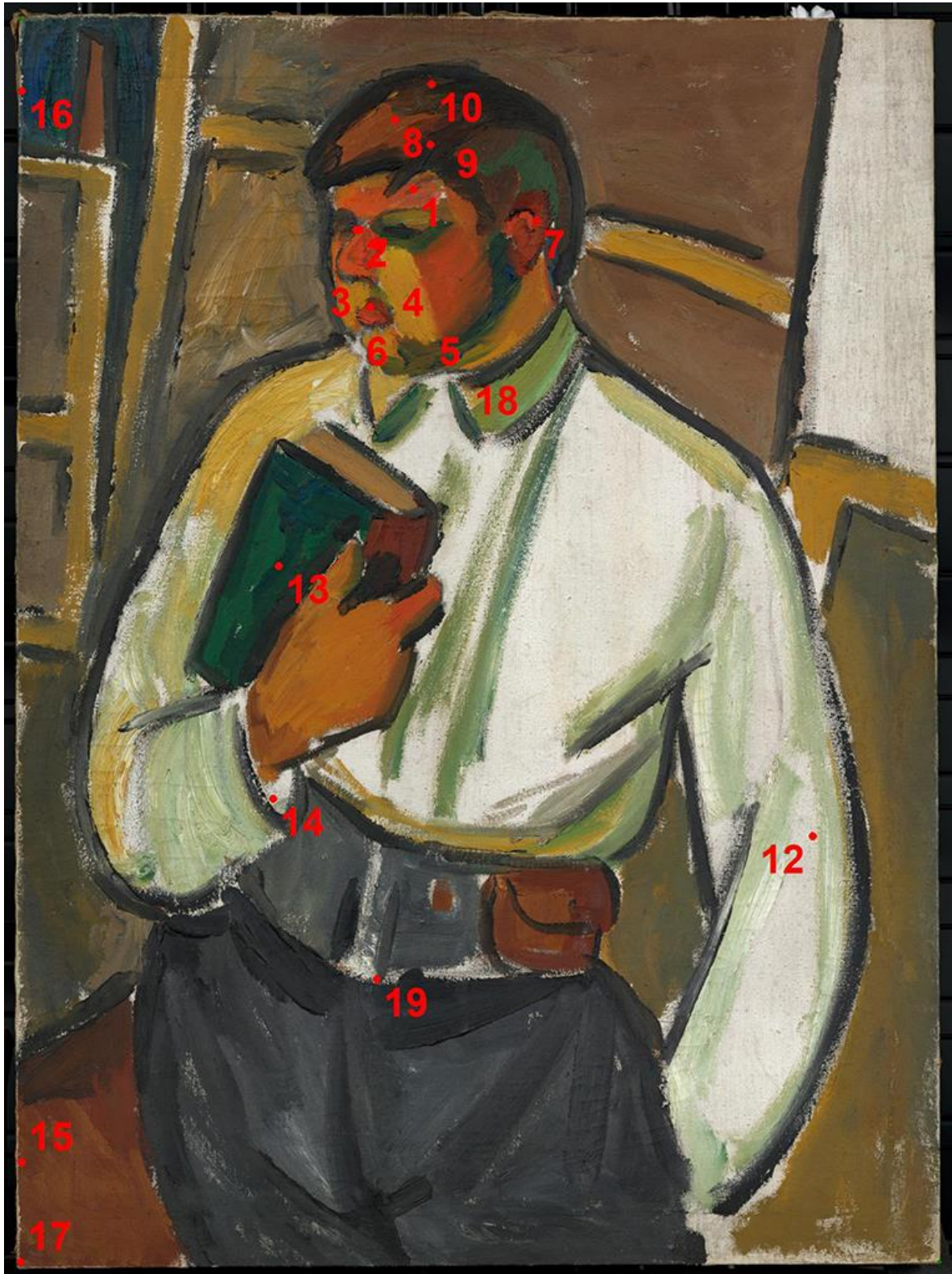


Plate 15. Image showing approximate location of samples taken for materials analysis.

App.5 Cross-sections³²



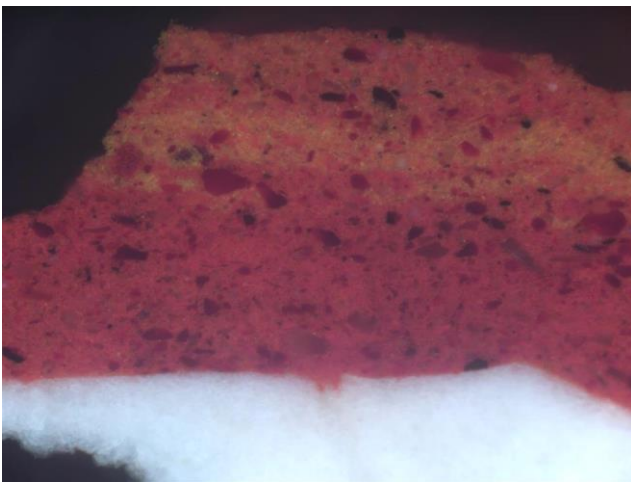
a.



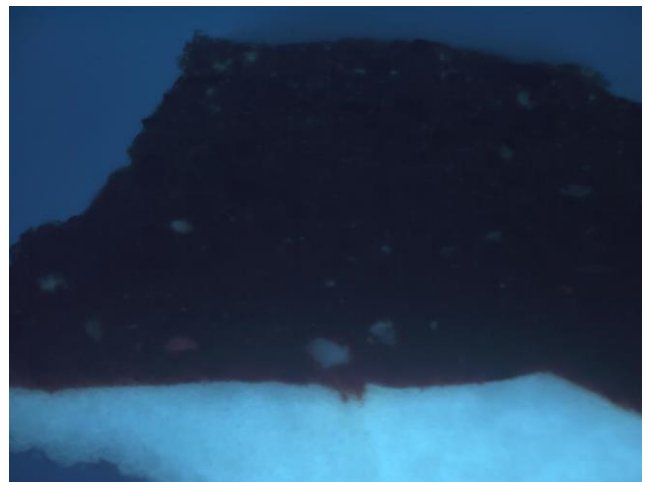
b.

Plate 16. Cross-section, Sample [15].

Image ~1mm high. Brown. White ground layer covered with a thick red-brown layer containing large red and colourless particles, and a few black particles. A yellow-orange paint is partially mixed in to the top part of this layer.



a.

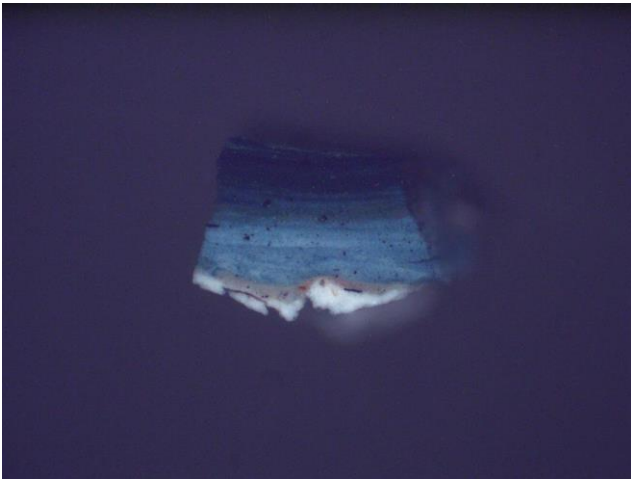


b.

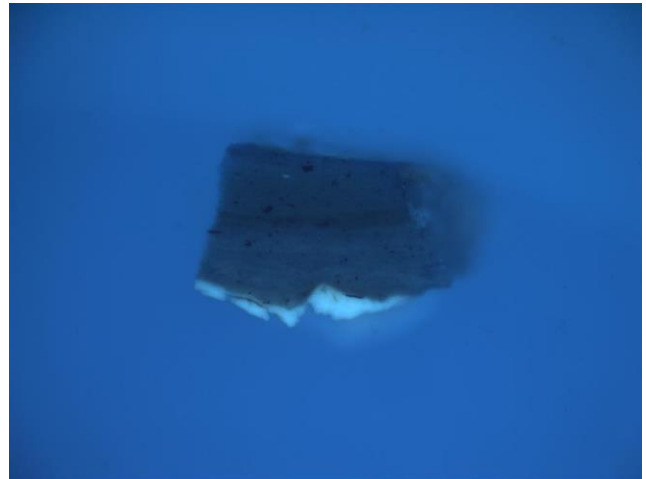
Plate 17. Cross-section, Sample [15].

Image ~260 μ m high. Brown, detail at higher magnification. One large red particle near the base of the red-brown layer displays pink luminescence under UV illumination.

³² Photographed under visible light, left (a.), and with ultraviolet illumination, right (b.) unless otherwise stated.



a.



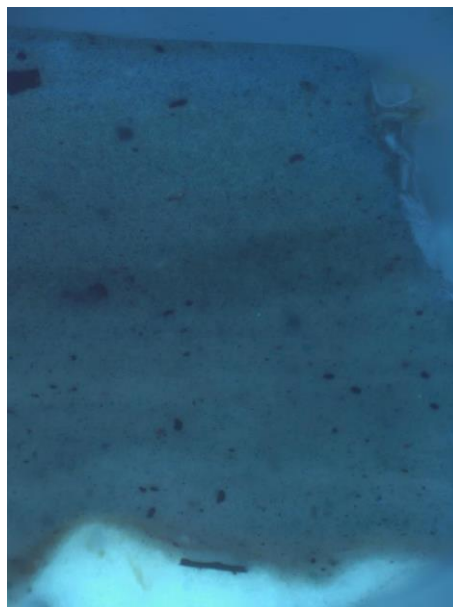
b.

Plate 18. Cross-section, Sample [16].

Image ~1mm high. Lowermost, white ground layer at base of sample, which is covered by a thin pale brown layer containing red, black and green particles, including one very large black splinter (relating to the underdrawing). A very thick, striated overall paint layer, applied wet-in-wet with no clear boundaries sits above. The lower portion is pale blue including some black and red particles. Halfway up is a green-blue band including a larger proportion of yellow particles, and the upper regions are darker blue, also including yellow, red and black particles.



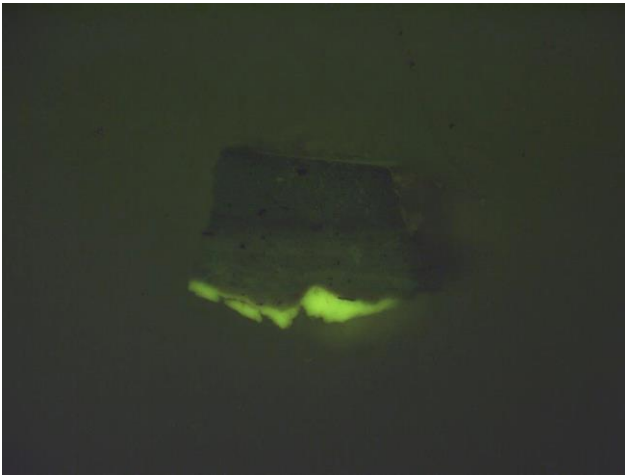
a.



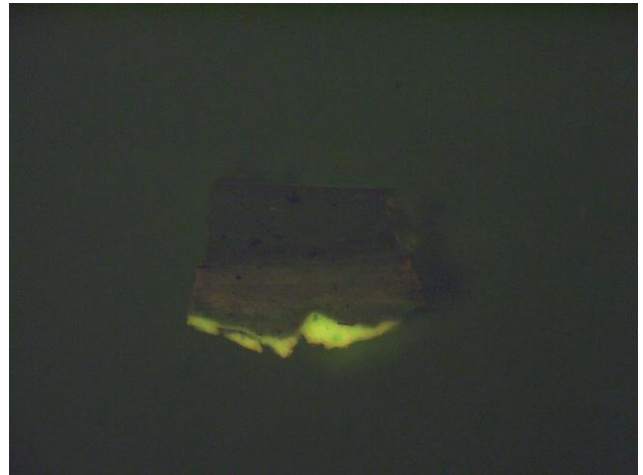
b.

Plate 19. Cross-section, Sample [16].

Image ~350µm high. Blue, detail at higher magnification.



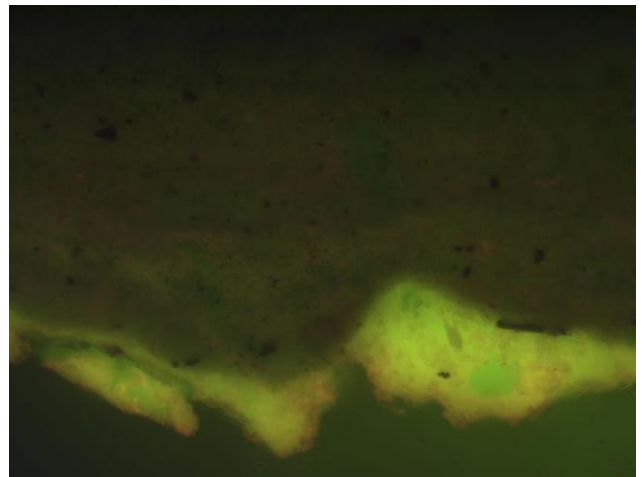
a.



b.

Plate 20. Cross-section, Sample [16], stained with SYPRO[®] Ruby.

Image ~1mm high viewed with Leica I3 filter before (left) and after (right) staining. Patchy pink staining of ground layer is visible, as well as pink staining of light and dark blue paint (lowest part of blue layer probably stained to a lesser extent). This probably indicates some protein present in the ground layer as well as some protein present in certain paint layers. Below, c.), at higher magnification.



c.